Phys Chem Minerals (2013) 40:447–453
DOI 10.1007/s00269-013-0582-8

ORIGINAL PAPER

Stability and equation of state of post-aragonite $BaCO_3$

Joshua P. Townsend · Yun-Yuan Chang · Xiaoting Lou · Miguel Merino · Scott J. Kirklin · Jeff W. Doak · Ahmed Issa · Chris Wolverton · Sergey N. Tkachev · Przemyslaw Dera · Steven D. Jacobsen

Received: 14 September 2012 / Accepted: 27 February 2013 / Published online: 16 March 2013

Abstract At ambient conditions, witherite is the stable form of $BaCO_3$ and has the aragonite structure with space group *Pmcn*. Above ~10 GPa, $BaCO_3$ adopts a post-aragonite structure with space group *Pmmn*. High-pressure and high-temperature synchrotron X-ray diffraction experiments were used to study the stability and equation of state of post-aragonite $BaCO_3$, which remained stable to the highest experimental *P–T* conditions of 150 GPa and 2,000 K. We obtained a bulk modulus $K_0 = 88(2)$ GPa with $K' = 4.8(3)$ and $V_0 = 128.1(5)$ Å^3 using a third-order Birch-Murnaghan fit to the 300 K experimental data. We also carried out density functional theory (DFT) calculations of enthalpy (*H*) of two structures of $BaCO_3$ relative to the enthalpy of the post-aragonite phase. In agreement with previous studies and the current experiments, the calculations show aragonite to post-aragonite phase transitions at ~8 GPa. We also tested a potential high-pressure post–post-aragonite structure (space group $C222_1$) featuring four-fold coordination of oxygen around carbon. In agreement with previous DFT studies, ΔH between the $C222_1$ structure and post-aragonite (*Pmmn*) decreases with pressure, but the *Pmmn* structure remains energetically favorable to pressures greater than 200 GPa. We conclude that post–post-aragonite phase transformations of carbonates do not follow systematic trends observed for post-aragonite transitions governed solely by the ionic radii of their metal cations.

Keywords $BaCO_3$ · Carbonates · High pressure · Equation of state

J. P. Townsend (✉) · Y.-Y. Chang · X. Lou · M. Merino · S. D. Jacobsen
Department of Earth and Planetary Sciences, Northwestern University, 2145 Sheridan Rd., Evanston, IL 60208, USA
e-mail: joshua@earth.northwestern.edu

S. J. Kirklin · J. W. Doak · A. Issa · C. Wolverton
Department of Materials Science and Engineering, Northwestern University, Evanston, IL 60208, USA

S. N. Tkachev · P. Dera
Argonne National Laboratory, Center for Advanced Radiation Sources, The University of Chicago, Argonne, IL 60439, USA

Introduction

The high-pressure and high-temperature behavior of carbonate minerals are important for modeling the Earth's global carbon cycle. Through subduction processes, carbonate-rich sediments are carried into the mantle, where partial melting returns a significant flux of CO_2 to the atmosphere through surface volcanism (e.g. Marty and Tolstikhin 1998; Fischer 2008). High-pressure phase transformations of carbonates have been extensively studied because of their potential to host carbon in the Earth's deep mantle (e.g. Boulard et al. 2011; Oganov et al. 2006; Isshiki et al. 2004; Ono et al. 2007; Merlini et al. 2012). Carbonate minerals are also considered potential host phases in CO_2 sequestration technology (e.g. Boulard et al. 2011; Giammar et al. 2005; Goff and Lackner 1998; O'Connor et al. 2002). The larger ionic radius of Ba^{2+} compared with Pb^{2+}, Sr^{2+}, Ca^{2+}, and Mg^{2+} has led to the expectation that $BaCO_3$ should undergo similar phase transitions, but at lower pressures than $PbCO_3$, $SrCO_3$, $CaCO_3$, or $MgCO_3$ (Liu and Bassett 1986; Lin and Liu 1997b; Santillán and Williams 2004). To further investigate predicted high-pressure structures and trends among carbonates containing different metal cation radii, we have studied the high-pressure behavior of $BaCO_3$ up to 150 GPa and 2,000 K, which was previously investigated experimentally to a maximum pressure of 75 GPa and temperature of 1,500 K (Ono 2007).

The calcite to aragonite transition of $CaCO_3$ occurs at pressures above ~2 GPa at high temperature (Suito et al. 2001) but exhibits a number of metastable polymorphs in the 1–15 GPa range along the 300 K compression path, including calcite-II (Merrill and Bassett 1975) and the recently solved structures of calcite-III and calcite-IV (Merlini et al. 2012). The orthorhombic (*Pmmn*) post-aragonite structure of $CaCO_3$ occurs at pressures above ~40 GPa and has been observed up to 140 GPa after heating to 1,700 K in experiments (Ono et al. 2007). The same study by Ono et al. (2007) showed that from 140 to 180 GPa, laser-heated $CaCO_3$ samples transformed to the pyroxene-type ($C222_1$) structure predicted by Oganov et al. (2006) from first principles.

$PbCO_3$ exhibits metastable polymorphism during 300 K compression, with a transition from the aragonite structure to a $PbCO_3$-II structure with space group $P12_1/c1$ at around 8 GPa (Minch et al. 2010). The aragonite to post-aragonite transition was observed at 17 GPa and 35 GPa in $PbCO_3$ and $SrCO_3$, respectively (Lin and Liu 1997b).

Magnesite ($MgCO_3$) is trigonal (R-3c) at room pressure and has been observed to transform to an orthorhombic phase at 115 GPa and 2,200 K, but the structure and space group have yet to be determined experimentally (Isshiki et al. 2004). Recent DFT calculations by Oganov et al. (2008) indicated several energetically similar structures above 84 GPa, including a *C2/m* structure (phase-II) containing three-membered rings of carbonate tetrahedral and a $P2_1$ (phase-III) form of $MgCO_3$ above ~140 GPa. The absence of an orthorhombic post-aragonite structure in $MgCO_3$ is perhaps explained by the relatively small ionic radius of Mg^{2+}.

300 K compression of $BaCO_3$ shows a displacive transition from the aragonite structure (Fig. 1a) to a metastable trigonal structure with space group *P-31c* (Holl et al. 2000; Ono 2007) but readily transforms to post-aragonite (*Pmmn*) (Fig. 1b) upon heating at 9–10 GPa (Ono 2007; this study). The post-aragonite form of $BaCO_3$ is stable up to at least 75 GPa based upon experimental work by Ono et al. (2008). A study by Zaoui and Shahrour (2010) suggested that $BaCO_3$ transforms to the $C222_1$ post–post-aragonite structure (Fig. 1c) above ~77 GPa using inter-atomic potential calculations. However, a recent DFT study by Arapan and Ahuja (2010) predicted that $BaCO_3$ should remain in the post-aragonite (*Pmmn*) structure to at least 300 GPa. Here, we extend the pressure range over previous experiments to explore possible phase transformations in $BaCO_3$ similar to the $C222_1$ phase observed for $CaCO_3$ above ~140 GPa (Ono et al. 2007).

Here, we report the results of high-pressure high-temperature X-ray diffraction of $BaCO_3$ up to 150 GPa and 2,000 K and calculate a 300 K equation of state. We also present the results of a first principles DFT investigation of several proposed high-pressure structures of $BaCO_3$ over the same pressure range, which in agreement with our experiments and the results of Arapan and Ahuja (2010), demonstrates that the post-aragonite structure is favored over the proposed pyroxene-type $C222_1$ structure to at least 150 GPa.

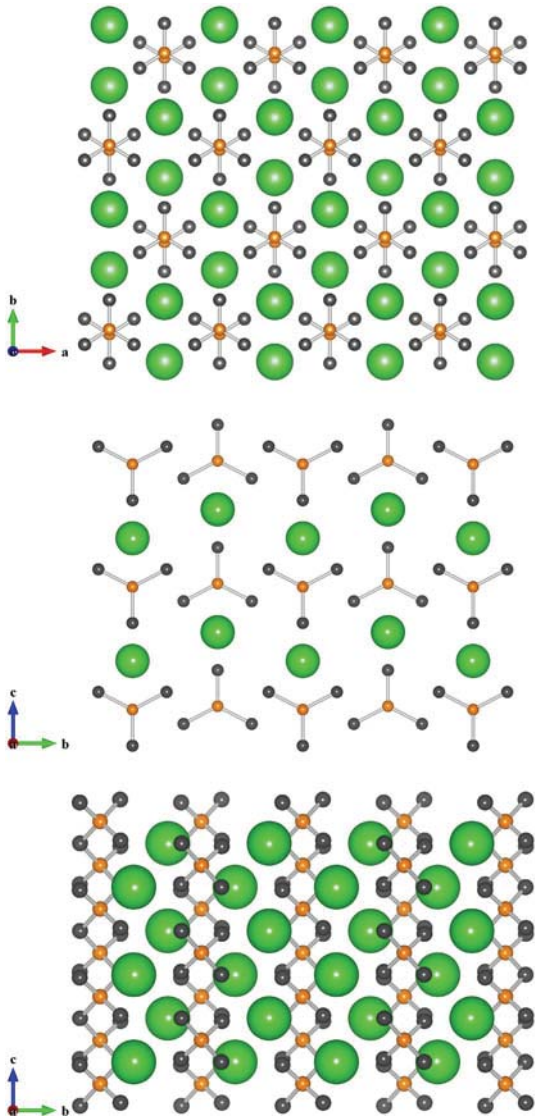

Fig. 1 High-pressure polymorphs of $BaCO_3$. Aragonite (*Pmcn*) (*top*) is stable under ambient conditions and features carbon in 3 coordination. Post-aragonite (*Pmmn*) (*middle*) is stable from ~9 GPa to at least 150 GPa. Post–post-aragonite ($C222_1$) (*bottom*) has not yet been observed experimentally, but features carbon in four-coordination. In all figures, the *large spheres* represent barium, the *small light spheres* represent carbon, and the *small dark spheres* represent oxygen

Experimental

Synchrotron X-ray diffraction

High-pressure X-ray diffraction experiments were performed at the Advanced Photon Source (APS), Sector 13

(GSECARS), beamline 13-ID-D. Platinum powder was incorporated into the witherite powder to act as a pressure standard and absorber for laser annealing. The sample was loaded into symmetric-type diamond anvil cell with beveled anvil culets of 100 μm inner diameter and 300 μm outer diameter. Neon was loaded as the pressure medium using the COMPRES/GSECARS gas-loading system at the APS (Rivers et al. 2008). Double-sided laser heating of the sample was accomplished using two 100 W, 1064 nm fiber lasers (IPG-Photonics YLR-series) with beam-shaping optics to produce a flat top laser heating area of approximately 15 × 15 μm (Prakapenka et al. 2008). Temperature was measured by the spectroradiometric method. X-ray diffraction patterns were collected using monochromatic X-rays of wavelength 0.3344 Å on a MAR-CCD detector. The focused X-ray beam area was about 5 × 5 μm at the sample. X-ray diffraction images were integrated to produce one-dimensional X-ray diffraction patterns using the Fit2d software (Hammersley et al. 1996). Pressures were calculated from the lattice parameters of platinum using the equation of state from Holmes et al. (1989). Diffracted peak positions were determined using the PeakFit software by Jandel Scientific. Lattice parameters of post-aragonite were refined using the program Unit Cell (Holland and Redfern 1997).

Density functional theory calculations

Density functional theory calculations were performed with the Vienna *Ab-initio* Simulation Package (VASP) using an energy cutoff of 500 eV. K-point meshes were generated using the Alloy Theoretic Advanced Toolkit (ATAT) (van de Walle et al. 2002) to produce 3,000 k-points per reciprocal atom in the Monkhorst–Pack scheme (Monkhorst and Pack 1976). Projector augmented wave potentials (Kresse 1999) were used in the Generalized Gradient Approximation (GGA) as parameterized by Perdew, Burke, and Ernzerhof (Perdew et al. 1996), with projection operators evaluated in real space. High-pressure calculations were done by incrementally increasing the pressure, using the previously relaxed structure as the input for the next pressure. All structures were fully relaxed using the conjugate gradient method. Gaussian smearing was used with a sigma value of 0.1 eV. Relative energies were converged to within 1 meV/atom with respect to energy cutoffs and k-points. All initial crystal structures were obtained from Oganov et al. (2006), Ono (2007), and the Inorganic Crystal Structure Database (ICSD).

Results and discussion

In the X-ray diffraction study, we recorded diffraction patterns before, during, and after heating (at 1,000–2,000 K) at pressures between approximately 1 and 150 GPa to explore possible phase transformations and to determine the equation of state of $BaCO_3$. At 9.1 GPa, we observed witherite (*Pmcn*) transform to the post-aragonite structure (*Pmmn*) after heating to ~1,100 K for 15 s. Figure 2 shows a representative X-ray diffraction pattern of post-aragonite measured at 9.1 GPa with peaks labeled for $BaCO_3$ post-aragonite, diamond, platinum, neon, and one unknown peak that did not belong to witherite, post-aragonite, diamond, platinum, or neon. The un-indexed peak disappeared upon increasing to the next pressure (16 GPa) and could have been due to a small amount of the metastable, trigonal *P-31c* structure observed on cold compression above 8 GPa by Holl et al. (2000). Fitted *d*-spacings at 9.1 GPa for the post-aragonite $BaCO_3$ structure are presented in Table 1 and agree well with previous experiments (Ono 2007).

Between ~10 and ~150 GPa, the $BaCO_3$ sample was heated for up to 20 min at up to 2,000 K, but no further phase changes were observed up to the maximum pressure of ~150 GPa. Specifically, we did not observe the $C222_1$ pyroxene-like structure predicted for $BaCO_3$ at 77 GPa by Zaoui and Shahrour (2010). The current experimental results demonstrate that $BaCO_3$ persists as post-aragonite (*Pmmn*) to at least 150 GPa, in agreement with predictions made by DFT (Arapan and Ahuja 2010).

Variation of the post-aragonite $BaCO_3$ lattice parameters up to ~150 GPa is shown in Fig. 3 and listed in Table 2. The *a*-axis, which is oriented perpendicular to the plane of the carbonate groups, is the most compressible. Up to 75

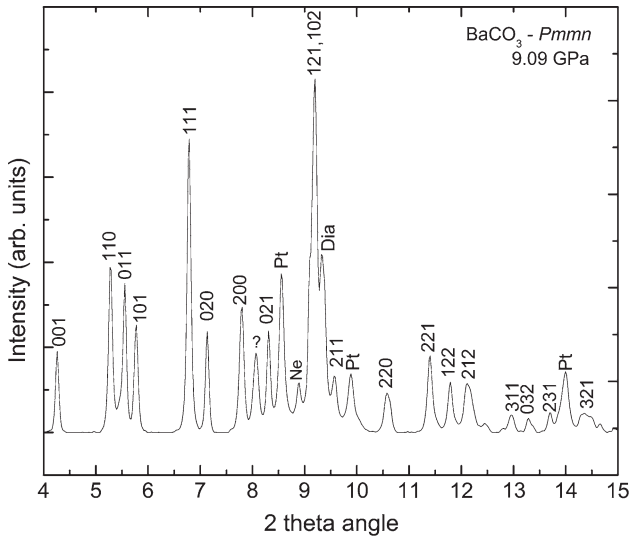

Fig. 2 X-ray diffraction pattern of post-aragonite $BaCO_3$ at 9.1 GPa after laser annealing at 1,100 K for 15 s. The single un-indexed peak labeled (?) could not be indexed as platinum (used as a laser absorber), rhenium (gasket), or neon (pressure medium), and may be due to a small amount of the trigonal $BaCO_3$ phase as reported by Holl et al. (2000). The unknown *peak* was observed at only a single pressure point

Table 1 Observed and calculated *d*-spacings for post-aragonite $BaCO_3$ at 9.1 GPa and 300 K after laser annealing at 1,100 K

hkl	d_{obs}	d_{calc}	$(d_{obs}/d_{calc})-1$
001	4.5004	4.5043	−0.0009
110	3.6290	3.6283	0.0002
011	3.4526	3.4518	0.0002
101	3.3208	3.3220	−0.0004
111	2.8580	2.8256	0.0002
020	2.6880	2.6866	0.0005
200	2.4604	2.4596	0.0003
021	2.3079	2.3073	0.0003
121	2.0886	2.0889	−0.0001
211	2.0042	2.0031	0.0005
220	1.8119	1.8141	−0.0012
221	1.6935	1.6828	0.0064
122	1.6285	1.6286	0.0001

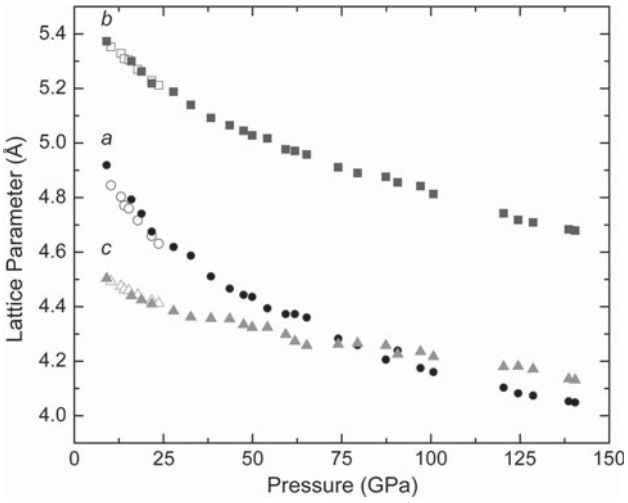

Fig. 3 Variation of the lattice parameters of post-aragonite $BaCO_3$ with pressure. *Open symbols* are data from Ono (2007), and *solid symbols* are from the current study

GPa, $a > c$, but above 75 GPa, $a < c$. The crossover of a and c lattice parameters at ~75 GPa is in agreement with DFT predictions by Arapan and Ahuja (2010). There is larger uncertainty in the a-axis at pressures between 50 and 80 GPa due to overlapping of the $BaCO_3$ post-aragonite (200) peak and the platinum (111) peak in the X-ray diffraction patterns, shown in Fig. 4. Overlap of the (110) and (011) peaks started to occur at approximately 50 GPa. Convergence of the (110) and (011) peaks was first reported by Ono (2007) and was originally thought to be evidence of a orthorhombic to tetragonal structure phase transition but was later shown not to be the case (Ono et al. 2008).

During the X-ray diffraction experiment, the sample was laser heated at up to 2,000 K for 10–20 min at every other pressure step to test for possible phase transitions and to anneal deviatoric stress in the sample chamber. Pressure–volume data measured after laser annealing were used to fit a 300 K third-order Birch-Murnaghan equation of state (Birch 1947; Angel 2001) (Eq.1):

$$P = 3K_0 f_E(1+2f_E)^{5/2}\left(1+\frac{3}{2}(K'-4)f_E\right) \quad (1)$$

where f_E is the Eulerian strain given by Eq. 2,

$$f_E = \frac{1}{2}\left[(V_0/V)^{2/3}-1\right] \quad (2)$$

and K_0 is the zero-pressure bulk modulus, and $K' = \frac{dK}{dP}$.

Fitted equation of state parameters to the data listed in Table 2 for post-aragonite $BaCO_3$ are $V_0 = 128.1(5)$ Å^3, $K_0 = 88(2)$ GPa, and $K' = 4.8(3)$. The zero-pressure bulk modulus and volume are in good agreement with Ono (2007), who obtained $K_0 = 84(4)$ GPa and $V_0 = 129.0(7)$ Å^3 using a second-order fit with $K' = 4$ (fixed). The volume–pressure data from this study and Ono (2007) are plotted in Fig. 5, along with the fitted 3rd order

Table 2 Pressure dependence of lattice parameters for post-aragonite $BaCO_3$ measured at 300 K

P (GPa)	*a* (Å)	*b* (Å)	*c* (Å)	Vol. (Å^3)
9.09	4.9192(4)	5.3731(5)	4.5043(6)	119.05(1)
16.01	4.7934(4)	5.3003(5)	4.4440(5)	112.91(1)
18.85	4.7410(4)	5.2622(5)	4.4249(5)	110.39(1)
21.73	4.6751(4)	5.2190(4)	4.4097(4)	107.59(1)
27.83	4.6187(4)	5.1885(5)	4.3843(4)	105.07(1)
32.71	4.5872(9)	5.1400(6)	4.3634(6)	102.88(2)
38.33	4.5106(5)	5.0924(5)	4.3571(5)	100.08(1)
43.61	4.4656(4)	5.0654(5)	4.3554(5)	98.52(1)
47.47	4.4433(5)	5.0452(5)	4.3340(6)	97.16(1)
49.88	4.4361(5)	5.0282(5)	4.3243(6)	96.45(1)
54.13	4.3939(6)	5.0171(5)	4.3242(6)	95.32(1)
59.29	4.3727(4)	4.9768(5)	4.2979(7)	93.53(1)
61.85	4.3727(7)	4.9708(5)	4.2728(7)	92.87(1)
65.20	4.3599(7)	4.9578(5)	4.2579(7)	92.04(1)
74.01	4.2829(9)	4.9110(5)	4.2615(6)	89.64(1)
79.42	4.2591(5)	4.8904(5)	4.2663(7)	88.86(1)
87.38	4.2056(8)	4.8761(5)	4.2582(6)	87.32(1)
90.70	4.239(1)	4.8560(5)	4.2257(8)	86.99(2)
97.08	4.1751(8)	4.8419(5)	4.2348(6)	85.61(1)
100.70	4.1595(4)	4.8131(5)	4.2169(7)	84.42(1)
116.73	4.1182(4)	4.7750(5)	4.1938(5)	82.47(1)
120.39	4.1033(3)	4.7418(5)	4.1799(4)	81.33(1)
124.47	4.0821(3)	4.7177(5)	4.1813(4)	80.52(1)
128.66	4.0739(3)	4.7093(5)	4.1712(4)	80.03(1)
136.44	4.0435(3)	4.6771(5)	4.1468(4)	78.43(1)
138.65	4.0533(4)	4.6825(6)	4.1347(6)	78.48(1)
140.43	4.0487(4)	4.6794(5)	4.1311(6)	78.27(1)

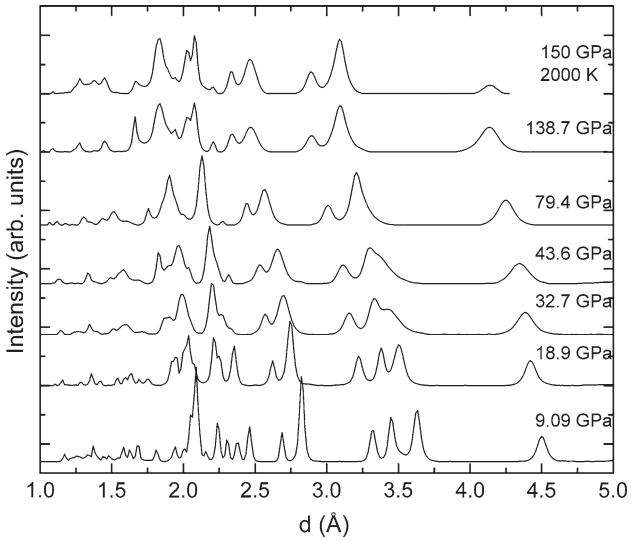

Fig. 4 X-ray diffraction patterns of post-aragonite $BaCO_3$ up to 140 GPa at 300 K. The pattern collected at 150 GPa and 2,000 K illustrates that no phase change has occurred. The merging of the (110) and (011) *peaks* is due to the crossing of the *a* and *c* lattice parameters but does not indicate a phase transition

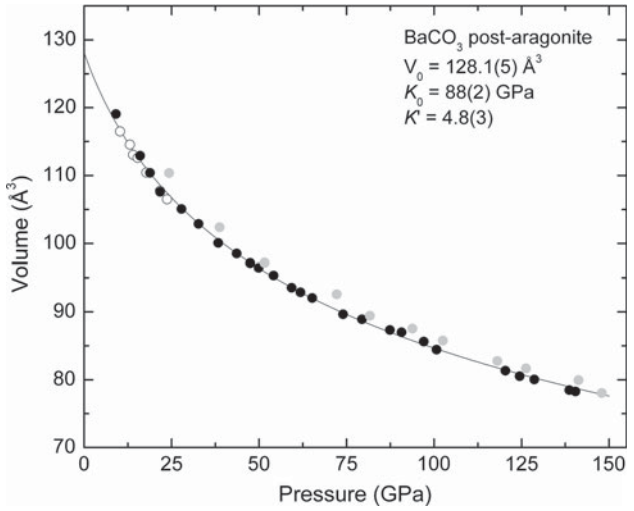

Fig. 5 Pressure–Volume equation of state of post-aragonite $BaCO_3$. *Open symbols* are from Ono (2007), filled *black symbols* were measured at 300 K, and *grey symbols* were measured at various high temperatures of 1,200–2,000 K

Birch-Murnaghan equation of state (solid line) resulting from this study. Because the lowest pressure of post-aragonite $BaCO_3$ is ~9 GPa, we tested our zero-pressure reference equation of state parameters by an alternative fitting method where we used 9 GPa as the reference pressure. Fitting all our data to a third-order equation of state with $P_{ref} = 9$ GPa, we obtain $V_{9GPa} = 117.8(5)$ Å^3, $K_{9GPa} = 128(7)$ GPa, and $K'_{9GPa} = 4.6(2)$. Extrapolating this equation of state back to 0 GPa, we obtain zero-pressure parameters of $V_0 = 128.3$ Å^3, $K_0 = 85$ GPa, and $K' = 5.1$, in good agreement with the standard reference fitting. A comparison of equation of state parameters from this and other studies is summarized in Table 3.

Table 3 Equation of state parameters for post-aragonite $BaCO_3$

Fitted EoS parameter	This study (exp) P_0 ref.	This study (exp) 9 GPa ref.	Ono (2007) (exp)	Ono et al. (2008) (calc)	Zaoui and Shahrour (2010) (calc)
V_0 (Å^3)	128.1(5)	128.3	129.0(7)	138.48	132.80
K_0 (GPa)	88(2)	85	84(4)	60.66	65.56
K'	4.8(3)	5.1	4.0 (fixed)	4.83	4.0 (fixed)

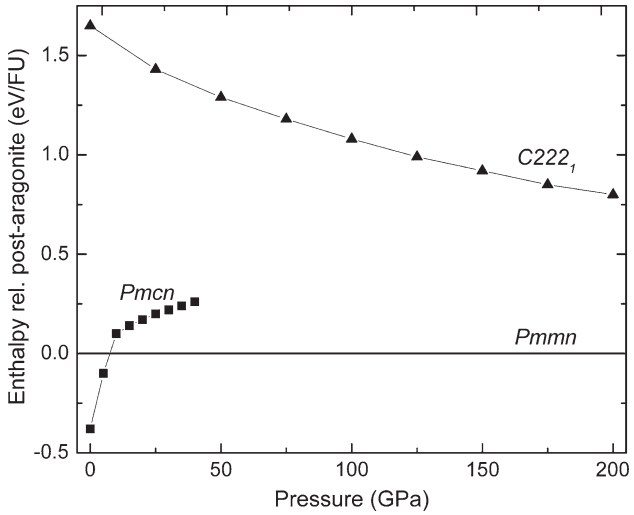

Fig. 6 Calculated enthalpy relative to post-aragonite $BaCO_3$. The *Pmmn* phase is energetically favorable up to at least 200 GPa, when compared to witherite *Pmcn* and post–post-aragonite $C222_1$

Figure 6 shows calculated enthalpies of aragonite-structured $BaCO_3$ (*Pmcn*) and the $C222_1$ structure (Oganov et al. 2006; Ono et al. 2007) relative to post-aragonite (*Pmmn*). Our calculations produce a witherite to post-aragonite transition pressure of 7.5 GPa, in good agreement with previous DFT studies (Ono et al. 2008; Arapan and Ahuja 2010) and the observed transition at ~9 GPa in our X-ray diffraction study. Unlike for $CaCO_3$ (Oganov et al. 2006; Ono et al. 2007), our calculations indicate that the $C222_1$ structure is not favored over post-aragonite for $BaCO_3$ over the entire experimental pressure range. This result does not agree with the inter-atomic potential calculations done by Zaoui and Shahrour (2010), which showed a post-aragonite to $C222_1$ transition at 76.7 GPa. The 'over-compressed' *Pmcn*-2 phase was not considered in this study because it was not stable within the experimental pressure range (Arapan and Ahuja 2010). The fact that no post-aragonite to post–post-aragonite phase transition was observed below ~150 GPa and 2,000 K is

somewhat surprising given the phase transition trajectories of other carbonates such as $CaCO_3$, for which the post-aragonite to post–post-aragonite transition has been experimentally observed (Ono et al. 2007).

Because $CaCO_3$ is observed to undergo a post-aragonite to post–post-aragonite transition (i.e., the $C222_1$ pyroxene-type structure), the expected transition pressure for $BaCO_3$ post-aragonite to post–post-aragonite was expected to occur at lower pressure, as predicted by Zaoui and Shahrour (2010). The absence of such a post–post-aragonite transition observed and calculated in this study calls into question the predicted crystal chemical systematics of carbonate transitions at ultra-high pressures.

In summary, we present X-ray diffraction experiments to 150 GPa and up to 2,000 K which show no further phase transformations following the transition from aragonite to post-aragonite at ~10 GPa. We show that the lattice parameters of the *a* and *c* axes meet at approximately 75 GPa. Crossover of the *a* and *c* lattice parameters coincides with the overlap of the (110) and (011) peaks, and separation of the two peaks was not observed upon further pressure increase. The post-aragonite (*Pmmn*) phase best describes all of the X-ray diffraction patterns up to ~150 GPa. DFT calculations further support that the post-aragonite phase is energetically favorable over the pyroxene-like $C222_1$ structure to at least 200 GPa.

Acknowledgments This research was supported by the NSF EAR-074787 (CAREER), the Carnegie/DOE Alliance Center (CDAC), and by the David and Lucile Packard Foundation to SDJ. Portions of this work were performed at GeoSoilEnviroCARS (GSECARS), Sector 13, Advanced Photon Source (APS), Argonne National Laboratory. GSECARS is supported by the NSF EAR-0622171 and Department of Energy DE-FG02-94ER14466. Use of the APS was supported by the DOE Office of Science, Office of Basic Energy Sciences, under Contract No. DE-AC02-06CH11357. This research was partially supported by COMPRES, the Consortium for Materials Properties Research in Earth Sciences under NSF Cooperative Agreement EAR 11-57758. SK was supported by the Center for Electrical Energy Storage: Tailored Interfaces, an Energy Frontier Research Center funded by the U.S. Department of Energy, Office of Science and Office of Basic Sciences. AI was supported by the Ford-Boeing-Northwestern (FBN) alliance, award no. 81132882. JWD was supported by the Revolutionary Materials for Solid State EnergyConversion, an Energy Frontier Research Center funded by the U.S. Department of Energy, Office of Science, Office of Basic Energy Sciencesunder Award Number DE-SC00010543.

References

Angel RJ (2001) Equations of state. In: Hazen, R.M., Downs, R.T. (eds) High-pressure, high-temperature crystal chemistry. Reviews in Mineralogy and Geochemistry, 41, 35–60

Arapan S, Ahuja R (2010) High-pressure phase transformations in carbonates. Phys Rev B 82:184115

Birch F (1947) Finite elastic strain of cubic crystals. Phys Rev 71:809–824

Boulard E, Gloter A, Corgne A, Antonangeli D, Auzende A-L, Perrillat J-P, Guyot F, Fiquet G (2011) New host for carbon in the deep Earth. Proc Nat Acad Sci 108:5184–5187

Fischer TP (2008) Fluxes of volatiles (H_2O, CO_2, N_2, Cl, F) from arc volcanoes. Geochem J 42:21–38

Giammar DE, Bruant RG, Peters CA (2005) Forsterite dissolution and magnesite precipitation at conditions relevant for deep saline aquifer storage and sequestration of carbon dioxide. Chem Geol 217:257–276

Goff F, Lackner KS (1998) Carbon dioxide sequestering using ultramafic rocks. Environ Geosci 5:89–101

Hammersley AP, Svensson SO, Hanfland M, Fitch AN, Häusermann D (1996) Two-dimensional detector to idealized image or two-theta scan. High Press Res 14:235–245

Holl CM, Smyth JR, Laustsen HMS, Jacobsen SD, Downs RT (2000) Compression of witherite to 8 GPa and the crystal structure of $BaCO_3$ II. Phys Chem Miner 27:467–473

Holland TJB, Redfern SAT (1997) Unit cell refinement from powder diffraction data; the use of regression diagnostics. Mineral Mag 61:65–77

Holmes NC, Moriarty JA, Gathers GR, Nellis WJ (1989) The equation of state of platinum to 660 GPa (6.6Mbar). J Appl Phys 66:2962–2967

Isshiki M, Irifune T, Hirose K, Ono S, Ohishi Y, Watanuki T, Nishibori E, Takata M, Sakata M (2004) Stability of magnesite and its high-pressure form in the lowermost mantle. Nature 427:60–63

Kresse G, Joubert D (1999) From ultrasoft pseudopotentials to the projector augmented-wave method. Phys Rev B 59: 1758–1775

Lin C, Liu L (1997a) High pressure phase transformations in aragonite-type carbonates. Phys Chem Miner 24:149–157

Lin C, Liu L (1997b) Post-aragonite phase transitions in strontianite and cerussite—a high-pressure Raman spectroscopic study. J Phys Chem Solids 58:977–987

Liu L, Bassett WA (1986) Elements, Oxides, and Silicates: High-pressure phases with implications for the earth's interior. Oxford University Press, New York

Marty B, Tolstikhin IN (1998) CO_2 fluxes from mid-ocean ridges, arcs, and plumes. Chem Geol 145:233–248

Merlini M, Hanfland M, Crichton WA (2012) $CaCO_3$-III and $CaCO_3$-VI, high-pressure polymorphs of calcite: possible host structures for carbon in the Earth's mantle. Earth Planet Sci Lett 333–334:265–271

Merrill L, Bassett W (1975) The crystal structure of $CaCO_3$(II), a high-pressure metastable phase of calcium carbonate. Acta Crystallogr A B31:343–349

Minch R, Peters L, Ehm L, Knorr K, Siidra OI, Prakapenka V, Dera P, Depmeier W (2010) Evidence for the existence of a $PbCO_3$-II phase from high pressure X-ray measurements. Z Kristallogr 225:146–152

Monkhorst HJ, Pack JD (1976) Special points for Brillouin-zone integrations. Phys Rev B 13:5188–5192

O'Connor WK, Dahlin DC, Rush GE, Dahlin CL, Collins WK (2002) Carbon dioxide sequestration by direct mineral carbonation: process mineralogy of feed and products. Miner Metall Process 19:95–101

Oganov AR, Glass CW, Ono S (2006) High-pressure phases of $CaCO_3$: crystal structure prediction and experiment. Earth Planet Sci Lett 241:95–103

Oganov AR, Ono S, Ma Y, Glass CW, Garcia A (2008) Novel high-pressure structures of $MgCO_3$, $CaCO_3$, and CO_2 and their role in Earth's lower mantle. Earth Planet Sci Lett 273:38–47

Ono S (2007) New high-pressure phases in $BaCO_3$. Phys Chem Miner 34:215–221

Ono S, Kikegawa T, Ohishi Y (2007) High-pressure transition of $CaCO_3$. Am Mineral 92:1246–1249

Ono S, Brodholt JP, Price GD (2008) Phase transitions of $BaCO_3$ at high pressures. Mineral Mag 72:659–665

Perdew JP, Burke K, Ernzerhof M (1996) Generalized gradient approximation made simple. Phys Rev Lett 77:3865–3868

Prakapenka VB, Kubo A, Kuznetsov A, Laskin A, Shkurikhin O, Dera P, Rivers ML, Sutton SR (2008) Advanced flat top laser heating system for high pressure research at GSECARS: application to the melting behavior of germanium. High Press Res 28:225–235

Rivers M, Prakapenka VB, Kubo A, Pullins C, Holl C, Jacobsen SD (2008) The COMPRES/GSECARS gas-loading system for diamond anvil cells at the advanced photon source. High Press Res 28:273–292

Santillán J, Williams Q (2004) A high pressure X-ray diffraction study of aragonite and the post-aragonite phase transition in $CaCO_3$. Am Mineral 89:1348–1352

Suito K, Namba J, Horikawa T, Taniguchi Y, Sakurai N, Kobayashi M, Onodera A, Shimomura O, Kikegawa T (2001) Phase relations of $CaCO_3$ at high pressure and high temperature. Am Mineral 86:997–1002

Van de Walle A, Asta M, Ceder G (2002) The alloy theoretic automated toolkit: a user guide. Calphad 26:539–553

Zaoui A, Shahrour I (2010) Molecular dynamics study of high-pressure polymorphs of $BaCO_3$. Philos Mag Lett 90:689–697